Water and Energy Exchanges at Forests and a Grassland in Eastern Siberia Evaluated using a One-dimensional Land Surface Model

doi: 10.1175/1525-7541(2004)005<0504:WAEEAF>2.0.CO;2

Water and Energy Exchanges at Forests and a Grassland in Eastern Siberia Evaluated Using a One-Dimensional Land Surface Model

TAKESHI YAMAZAKI

Frontier Observational Research System for Global Change, Yokohama, and Department of Geophysics, Graduate School of Science, Tohoku University, Sendai, Japan

HIRONORI YABUKI

Frontier Observational Research System for Global Change, Yokohama, Japan

YOSHIYUKI ISHII

Institute of Low Temperature Science, Hokkaido University, Sapporo, Japan

TAKESHI OHTA

Graduate School of Bioagricultural Science, Nagoya University, Nagoya, and Frontier Observational Research System for Global Change, Yokohama, Japan

TETSUO OHATA

Institute of Low Temperature Science, Hokkaido University, Sapporo, and Frontier Observational Research System for Global Change, Yokohama, Japan

(Manuscript received 22 August 2003, in final form 18 January 2004)

ABSTRACT

Water and energy exchanges are evaluated for two larch forests, one pine forest, and one grassland area in eastern Siberia near Yakutsk using a one-dimensional land surface model. Diurnal and seasonal variations of fluxes are simulated reasonably with general stomatal parameters at all sites. In the grassland site, the Bowen ratio is 0.2 in midsummer; it is smaller than that in forest sites (about 1). Sensitivity tests indicate that leaf area should be given accurately along with total plant area index including stem and branch areas. If both plant and leaf areas are given, the outline of seasonal heat balance can be simulated using the same stomatal parameters for forests and grassland sites with the model.

In the larch site on the left bank of the Lena River, although input precipitation varies widely from 82 to 236 mm year to year from 1998 through 2000, calculated total evapotranspiration varies only within a range of 50 mm around 238 mm in the larch site. Understory evapotranspiration contributes 37%–44% to total evapotranspiration; interception is 15%–21% of precipitation. Evapotranspiration normalized by potential evaporation is 0.37 for larch sites almost independent of year; for grassland it is 0.52. At some sites, evapotranspiration in the warm season exceeds precipitation, thereby implying either a warm-season depletion of water storage in the soil column (most likely melted water from the thawing of the soil) or a horizontal transport of subsurface melt water from neighboring areas, or both.

1. Introduction

A vast taiga forest extends over northern Eurasia, including eastern Siberia. Although the taiga forest is often thought to be covered homogeneously by coniferous trees, there are many dispersed grasslands called ''alas.'' According to Suzuki et al. (2004), larch forests occupy about 61%, whereas pine forests are about 7%; however, nonforested areas (mainly grasslands and lakes) also reach 29% on the right bank (east side) of the Lena River and 14% on the left bank (west side) of the Lena River near Yakutsk, eastern Siberia. What are evapotranspiration differences between forests and grasslands? Kelliher et al. (1993) reviewed evaporation of coniferous forests and grasslands; they reported that evaporation is slightly larger in grasslands (daily basis, median value is 4.0 mm day^{-1} in forests and 4.6 mm day^{-1} in grasslands) even though surface conductances

Corresponding author address: Dr. Takeshi Yamazaki, Frontier Observational Research System for Global Change, 3173-25, Showa-machi, Kanazawa-ku, Yokohama 236-0001, Japan.
E-mail: yamaz@jamstec.go.jp

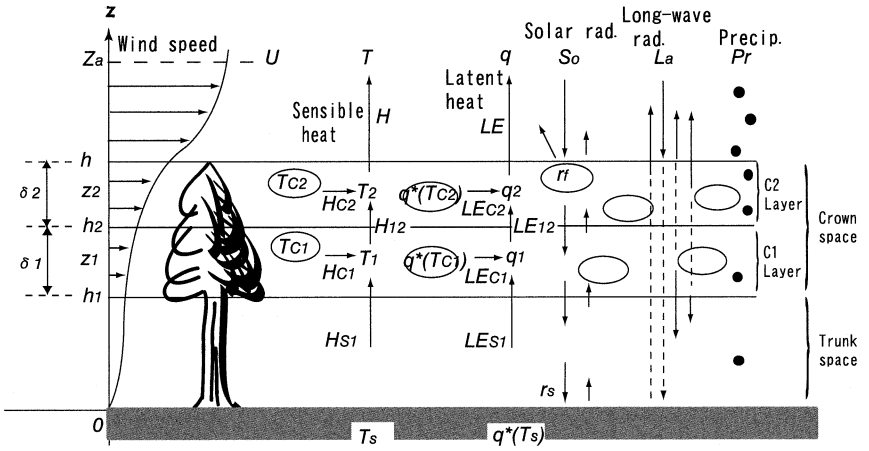

FIG. 1. A schematic diagram of the canopy submodel.

are similar. Garratt (1992) summarized resistances of various canopy types and found that the surface resistance of coniferous forests is larger than that of grassland. Eugster et al. (2000) summarized the surface energy balance of Arctic tundra and boreal forest; they showed maximum canopy conductance is small in light taiga. Baldocchi et al. (2000) also described that evaporation over conifer stands is relatively low and that from broad-leaved stands and fen/wetlands approaches equilibrium evaporation rates. Based on those findings, it is expected that evapotranspiration is greater in grasslands than in forests if climatic conditions are similar.

Meteorological and hydrological observations were carried out at a larch forest site since 1997 near Yakutsk (Ohta et al. 2001), as part of the Global Energy and Water Cycle Experiment (GEWEX) Asian Monsoon Experiment (GAME); GAME is a continental-scale experiment of GEWEX. Intensive observations were conducted during 2000 for various vegetation types (larch, pine, and grassland); data are now undergoing analysis from various perspectives. It has been found that evapotranspiration is greater in the grassland than in the larch forest. On the other hand, land surface schemes, virtually all of which have been developed in temperate zones, do not perform well in high-latitude regions. This report presents a one-dimensional land surface model to estimate energy and water exchange in intensely cold regions. The model was validated against 1998 larch forest data for Siberia (Yamazaki 2001). The model is physically based and includes three submodels: vegetation, snow cover, and soil. Diurnal and seasonal changes of fluxes were simulated reasonably at a larch forest site using this model.

This paper improves the model and applies it to various Siberian sites, focusing on water and energy exchanges. Our study emphasizes differences and similarities of model parameters between forests and grassland to explain observed seasonal flux variations. Another purpose of this study is the discussion of a water budget using model-calculated fluxes. It is very difficult to obtain high quality flux data for long periods, especially in high-latitude regions. The advantage of a model used to estimate a water budget is that missing flux observations can be interpolated if only forcing data are available. Important factors indicating the water budget of taiga forests in eastern Siberia are permafrost and understory evapotranspiration. In spite of low precipitation (average annual precipitation is 213 mm in Yakutsk), a taiga forest was established; thus it has been believed that permafrost serves an important function for existence of taiga in eastern Siberia. Sugimoto et al. (2002) recently clarified that permafrost played the role of providing water for vegetation in a severe drought summer through stable isotope measurements. The importance of understory evapotranspiration was confirmed in eastern Siberia taiga forests through observations (Kelliher et al. 1997; Ohta et al. 2001); it contributed 35%–50% to total evapotranspiration because of the low canopy density. We show that our model, which includes rather simple parameterization of these factors, can simulate the water budget. Finally, results will be discussed with reference to potential evaporation.

2. Model

The one-dimensional land surface model includes the following three submodels. Details of the model have been described in Yamazaki (2001), although liquid water flow in the soil layer is newly taken into account. Input data are wind speed, air temperature, specific humidity (or water vapor pressure), precipitation, solar shortwave radiation, and downward longwave radiation.

a. The canopy submodel

The basis of this submodel and its performance for 30-min runs were described by Yamazaki et al. (1992). Figure 1 shows the schematic diagram of the canopy submodel. The heat storage term and canopy intercep-

tion of rain were added by Yamazaki (2001). Fluxes above and in the canopy can be calculated with this model. The canopy is divided into a ''crown space'' and a ''trunk space'' (without leaves), with the crown space subdivided into two layers. The heat balance is resolved with respect to radiative, sensible, and latent heat fluxes among the atmosphere and the two crown layers. Sensible and latent heat fluxes are described as proportional to differences of temperature and specific humidity, respectively.

The heat-balance equation for each layer is

$$C\frac{dT_{Ci}}{dt} = S_{Ci} + L_{Ci} - H_{Ci} - LE_{Ci}, \quad (i = 1, 2), \quad (1)$$

where T_{Ci} is canopy temperature in ith layer (K), S_{Ci} and L_{Ci} are the net absorption of solar and infrared radiation, H_{Ci} and LE_{Ci} are the sensible and latent heat fluxes from the canopy elements to the surrounding air in the ith layer (units of all energy fluxes are watts per meter squared). The left-hand-side term is the heat storage term; C represents heat capacity (J m^{-2} K^{-1}).

Because the fluxes must be continuous,

$$H_{C1} = H_{12} - H_S, \quad (2)$$

$$H_{C2} = H - H_{12}, \quad (3)$$

$$LE_{C1} = LE_{12} - LE_S, \quad \text{and} \quad (4)$$

$$LE_{C2} = LE - LE_{12}. \quad (5)$$

Here, H and LE are sensible and latent heat fluxes from the top of the canopy layer to the atmosphere, H_{12} and LE_{12} are those between two canopy layers, and H_S and LE_S are those at the bottom of the canopy layer (equal to those over snow or the soil surface), respectively.

Evapotranspiration generated in layer i, E_{Ci}, is written as

$$E_{Ci} = \rho_a j_i c_h (a - a_{\min})\delta_i U_i [q_{\text{sat}}(T_{Ci}) - q_i], \quad (6)$$

where ρ_a is air density (kg m^{-3}), j_i shows the leaf evapotranspiration factor (dimensionless), and c_h is the transfer coefficient of individual leaves for sensible heat (dimensionless); a shows plant area density (m^{-1}) (=PAI′/δ, PAI′: effective plant area index, δ: thickness of crown space), $a_{\min} = \text{PAI}'_{\min}/\delta$, $\text{PAI}'_{\min}$ is the effective plant area index excluding leaves, δ_i is the thickness of each canopy layer (m), U_i and q_i are wind speed (m s^{-1}) and specific humidity in each canopy layer (kg kg^{-1}), and q_{sat} represents saturation specific humidity. Note that as a vegetation density, ''effective'' plant area index, PAI′, which does not consider clustered structure or concentration of crowns, is used in this model because leaves and branches are concentrated; therefore, they do not contribute to absorption of radiation, etc., effectively. It can be related to the ''actual'' plant area index, PAI, which is defined as the entire plant area over the unit ground surface obtained by direct measurement such as tree cutting, etc., as

$$\text{PAI}' = \lambda \text{PAI}. \quad (7)$$

Here, λ is the coefficient indicating leaf concentration (dimensionless); it corresponds to the reciprocal of shelter factor (e.g., Raupach and Thom 1981).

The evapotranspiration factor j (dimensionless) is written with use for stomatal resistance, r_s(s m^{-1}):

$$j = \frac{1}{1 + c_h U r_s}. \quad (8)$$

A hyperbolic relationship (e.g., Turner and Begg 1973) is used for stomatal resistance:

$$r_s = r_m(1 + S_{\text{abm}}/S_{\text{abi}})\Omega. \quad (9)$$

Here, S_{abi} represents shortwave radiation absorbed by a unit of leaf area in the ith layer, which is calculated in the model; r_m is the minimum value of r_s; and S_{abm} is the value of S_{abi} when $r_s = 2r_m$. The factor Ω expresses the influence of air dryness,

$$\Omega = 1/(1 - B \times \text{VPD}), \quad (10)$$

where VPD is the saturation deficit (hPa) and B is a coefficient depending on species (hPa^{-1}).

Canopy albedo is described with two parameters: α_f and α_s. Here, α_f is a parameter related to reflectance of canopy elements (leaf, branch, etc.), whereas α_s is forest floor or soil surface reflectance (dimensionless). In this study, $\alpha_f = C_1 C_* + C_2$ is assumed—where C_* is the nondimensional canopy density, and C_1 and C_2 are empirical coefficients—to address the seasonal development of canopy elements.

b. The snow-cover submodel

In this model, snow is treated as having multilayers with thickness of 0.02 m. The basic equation to solve the temperature profile in snow cover is

$$c_{\text{snow}}\rho_{\text{snow}}\frac{\partial T_{\text{snow}}}{\partial t} = \frac{\partial}{\partial z}\left(\lambda_{\text{snow}}\frac{\partial T_{\text{snow}}}{\partial z}\right) - \frac{\partial I_n}{\partial z} - L_f F, \quad (11)$$

where T_{snow} is snow temperature (K); c_{snow}, ρ_{snow}, and λ_{snow} are specific heat capacity (J kg^{-1} K^{-1}), density (kg m^{-3}), and thermal conductivity of snow (W m^{-1} K^{-1}); t is time (s); z is a vertical coordinate (m) (downward positive); I_n is net solar flux in the snow cover; L_f is latent heat of fusion (J kg^{-1}); and F is the amount of snowmelt per unit time and volume (kg m^{-3} s^{-1}) (when $T_{\text{snow}} < 0$°C, $F = 0$).

c. The soil submodel

Soil layers in this model have a thickness of 0.1 m except for the top layer (0.02 m). To calculate soil temperature, an equation similar to (11) is used,

$$c_{\text{soil}}\rho_{\text{soil}}\frac{\partial T_{\text{soil}}}{\partial t} = \frac{\partial}{\partial z}\left(\lambda_{\text{soil}}\frac{\partial T_{\text{soil}}}{\partial z}\right). \quad (12)$$

Heat of fusion of frozen soil is taken into account with a method in which heat capacity is regarded as larger in a small temperature range between T_1 and T_2 (set to $-1°$ and 0°C, respectively) according to Fukuda and Ishizaki (1980). The rate of soil water change is expressed as

$$\rho_w \frac{\partial \theta}{\partial t} = -\frac{\partial Q_{\mathrm{LIQ}}}{\partial z} - \frac{E_i + E_s + R_{\mathrm{off}}}{dz}. \quad (13)$$

Here, ρ_w represents liquid water density (kg m^{-3}), θ is volumetric soil water content (m^3 m^{-3}), Q_{LIQ} is liquid water flux (kg m^{-2} s^{-1}), E_t is transpiration (kg m^{-2} s^{-1}), E_s is evaporation from the soil (kg m^{-2} s^{-1}), and R_{off} is runoff (kg m^{-2} s^{-1}). At the bottom boundary of the model soil layers (at 10-m depth), soil temperature and water content are fixed at a climatic annual mean value.

Thermal conductivity of soil is assumed as

$$\lambda_{\mathrm{soil}} = 0.251 + 0.5\theta^{1/3} \quad (14)$$

for unfrozen soil. If the soil is frozen, λ_{soil} is set to 1.5 times the value obtained from (14). In the top layer of the soil, λ_{soil} is given a lower value of 0.3 W m^{-1} K^{-1} to account for the organic matter covering the ground.

The liquid water flux Q_{LIQ} is defined as

$$Q_{\mathrm{LIQ}} = -\rho_w K(\theta)\left(\frac{\partial \psi}{\partial \theta}\frac{\partial \theta}{\partial z} + \frac{\partial \psi}{\partial T}\frac{\partial T}{\partial z} - 1\right). \quad (15)$$

Here, $K(\theta)$ and $\Psi(\theta)$ are hydraulic conductivity (m s^{-1}) and matric potential (m), respectively. According to Clapp and Hornberger (1978), these two variables are given as

$$K(\theta) = K_{\mathrm{sat}}\left(\frac{\theta}{\theta_{\mathrm{sat}}}\right)^{2b+3} \quad \text{and} \quad (16)$$

$$\psi(\theta) = \psi_{\mathrm{sat}}\left(\frac{\theta}{\theta_{\mathrm{sat}}}\right)^{-b}. \quad (17)$$

Here, the subscript sat denotes the saturation-condition value, and b is a constant (dimensionless) depending on soil type. If soil is freezing or thawing, θ (including both liquid and ice water) is replaced by the unfrozen liquid water content; θ_l is assumed as

$$\theta_l = \begin{cases} \theta & (T > T_2) \\ (T - T_1)/(T_2 - T_1)\theta & (T_1 \le T \le T_2) \\ 0 & (T < T_1). \end{cases} \quad (18)$$

Thus, when $T < T_1$, $Q_{\mathrm{LIQ}} = 0$.

Transpiration, E_t, is distributed in the top three layers proportional to layer thickness. If soil is frozen ($T < T_2$) or $\theta < \theta_{\mathrm{wilt}}$, water is squeezed from the layer underneath; θ_{wilt} is volumetric water content at the wilting point assumed as the value corresponding to $\Psi = -150$ m. On the other hand, evaporation from the soil, E_s, is usually taken from the topmost layer. However, when soil is very dry ($\theta < 0.05$), water is taken from the next layer underneath. Runoff, R_{off}, is given as the sum of the water exceeding θ_{sat} in each layer; also, $\rho_w K_i \sin\alpha$ is added when soil moisture approaches saturation ($\theta > \theta_{\mathrm{sat}} - 0.05$), where α is the slope angle. This means that if water content in a certain layer reaches saturation, saturated subsurface flow is assumed to occur.

When no snow cover exists, the heat balance equation at the soil surface or forest floor,

$$(1 - A)S^{\downarrow} + \varepsilon(L^{\downarrow} - \sigma T_s^4) - H_S - LE_S + G_0 = 0, \quad (19)$$

should be considered. Here, A represents albedo, $S^{\downarrow}$ is downward solar radiation, ε is the emissivity of soil surface or forest floor, $L^{\downarrow}$ is downward longwave radiation, σ is the Stefan–Boltzmann constant, T_s is soil surface temperature, and H_s and LE_s are sensible and latent heat fluxes over the soil surface, written as

$$H_S = c_p \rho_a C_H U(T_s - T_a) \quad \text{and} \quad (20)$$

$$LE_S = L\rho_a \beta_{\mathrm{soil}} C_H U[q_{\mathrm{sat}}(T_s) - q_a]. \quad (21)$$

Here, c_p represents the specific heat of air, C_H is the bulk transfer coefficient for sensible heat (dimensionless), and U, T_a, and q_a are wind speed (m s^{-1}), air temperature (K), and specific humidity (kg kg^{-1}); L is latent heat of evaporation or sublimation (J kg^{-1}) and β_{soil} is moisture availability (dimensionless).

Soil moisture availability, β_{soil}, is given by the following two methods depending on site. In the first method β_{soil} is obtained from an empirical function of soil water content for bare soil (Kondo et al. 1990):

$$\beta_{\mathrm{soil}} = \left[1 + \frac{C_H U F(\theta)}{D_{\mathrm{atm}}}\right]^{-1}, \quad (22)$$

$$F(\theta) = F_1(\theta_{\mathrm{sat}} - \theta)^{F_2}. \quad (23)$$

Here, D_{atm} is the molecular diffusivity of water vapor (m^2 s^{-1}); F_1 and F_2 are experimental coefficients (meters and dimensionless, respectively) depending on soil type. The other method is to use the approach in Eq. (8) together with a ground surface resistance r_g,

$$\beta_{\mathrm{soil}} = \frac{1}{1 + C_H U r_g}. \quad (24)$$

In general, r_g depends on the water status of the understory vegetation.

3. Site and data

There are four sites around Yakutsk related to the GAME-Siberia project (Table 1). Two of them are young larch [hereafter, right larch (RL)] and grassland [right grass (RG)] sites located on the right bank of the Lena River. The other two are relatively old larch [left larch (LL)] and pine [left pine (LP)] sites on the left bank of the Lena River. Right-bank sites and left-bank sites are separated by 50 km; distances of RL–RG and LL–LP are 0.5 and 2.2 km, respectively. On the RG site, grass

TABLE 1. Site characteristics. Elevation is 150 m in RL and RG, 220 m in LL and LP.

Site	Lat, lon	Main species	Canopy height (m)	Tower or mast height (m)	Used data period
RL	62°09′N, 130°31′E	*Larix gmelinii*	10	23	16 Apr–11 Sep 2000
RG	62°09′N, 130°31′E	*Puccinellia tenuiflora*	0.5	2	17 Apr–11 Sep 2000
LL	62°15′N, 129°37′E	*Larix gmelinii*	18	32	21 Apr–15 Sep 1998 19 Apr–10 Sep 1999 19 Apr–4 Sep 2000
LP	62°14′N, 129°39′E	*Pinus sylvestris*	10	18	21 Apr–4 Sep 2000

was cut on 21 July 2000; in general, grass is cut once in summer in this region to produce feed.

As necessary drivers for the model, air temperature, humidity, and wind speed are observed at each site. Shortwave radiation and longwave radiation are measured except for RG; radiation data from RL are used in the model calculation for RG. Precipitation is observed at open spaces near the sites on both banks; therefore, common precipitation data is used for the two sites on each bank. Sensible, latent, and ground heat fluxes are measured or estimated by eddy covariance and Bowen ratio methods, which can be used to validate model simulations. Detailed site descriptions and observed elements can be found in Ishii (2001) and Yabuki (2001a,b) for the right bank and Ohta et al. (2001) and Hamada et al. (2004) for the left bank.

4. Results

a. Parameters and initial conditions

Diurnal and seasonal variations of fluxes were simulated for sites RL, RG, and LP in 2000, and for LL in 1998, 1999, and 2000. Main parameter values in simulations are listed in Table 2.

Parameters related to stomatal resistances, r_m, S_{abm}, and B are determined by trial and error to agree with the observed Bowen ratio (H/LE) and the seasonal variation of the fluxes. The reason that absolute values were not used to determine parameters is the so-called energy imbalance problem: observed fluxes do not satisfy the heat balance equation, even though it is satisfied exactly in the model. For example, $(H + LE)/(\mathrm{Rn} - G)$ is 0.75 in LL (Ohta et al. 2001), whereas it is 1.01 in LP where it depends on wind direction (Hamada et al. 2004). As a result, values of r_m and S_{abm} are identical values obtained in a previous LL1998 simulation (Yamazaki 2001) for all sites, independent of vegetation type (larch, pine, or grass) and year. The value of B is slightly larger in the pine site, whereas it is small in the grass site compared to larch sites.

Effective plant area index, PAI′, in forest sites is determined according to the ratio of solar radiation on the forest floor to that over the forest. Note that actual values of PAI are summarized in Toba and Ohta (2002) as 3.50 in RL, 3.71 (1.56 in leafless season) in LL, and 2.80 in LP. Thus, the corresponding λ are 0.31 in RL, 0.32 (0.51 in leafless season) in LL, and 0.43 in LP, respectively. For the RG site, parameters related to PAI are obtained from in situ measurements (H. Tanaka, H. Yabuki, and N. Kobayashi 2002, unpublished data) with $\lambda = 0.5$. After all, the seasonal change of PAI′ in RG is assumed as shown in Fig. 2 in consideration of grass cutting; however, PAI′ = 0 in the snow season. For the evergreen LP site, PAI′ is kept constant ($= \mathrm{PAI}_{max}$) in the simu-

TABLE 2. Parameter values used in simulations.

Parameter	Symbol	Unit	RL	RG	LL	LP
Min plant area index	PAI'_{min}	—	0.75	0.35	0.8	0.8
Max plant area index	PAI'_{max}	—	1.1	1.5	1.2	1.2
Canopy height	h	m	10	0.5	18	10
Canopy layer bottom height	h_1	m	5	0.25	9	5
Min stomatal resistance	r_m	s m^{-1}	50	50	50	50
Stomatal parameter on solar radiation	S_{abm}	W m^{-2}	150	150	150	150
Parameter for influence of air dryness	B	hPa^{-1}	0.027	0.020	0.027	0.035
Coef for canopy albedo	C_1	—	0.75	0.33	0.75	0
	C_2	—	−0.15	0	−0.15	0.13
Albedo of forest floor or soil surface	α_s	—	0.15	0.05	0.18	0.18
Saturation soil moisture	θ_{sat}	—	0.43	0.43	0.43	0.4
Matric potential (saturation)	ψ_{sat}	m	−0.218	−0.218	−0.218	−0.09
Hydraulic conductivity (saturation)	K_{sat}	m s^{-1}	3.47×10^{-5}	3.47×10^{-5}	3.47×10^{-5}	1.56×10^{-4}
Empirical const	b	—	4.9	4.9	4.9	4.38
Surface moisture availabiltiy	β_{soil}	—	Eq. (24)	Eq. (22)	Eq. (24)	Eq. (24)
	F_1	m	—	7.0×10^3	—	—
	F_2	—	—	11.2	—	—
	r_g	s m^{-1}	500	—	500	500

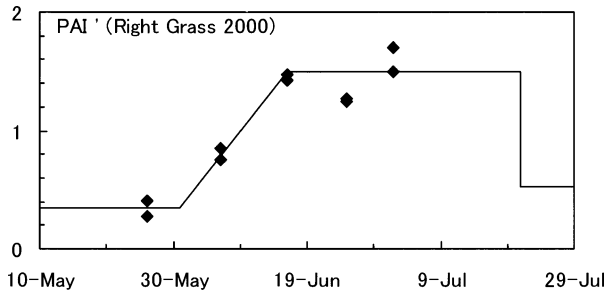

FIG. 2. Effective plant area index in RG. Diamonds are in situ data measured by leaf cutting (H. Tanaka, H. Yabuki, and N. Kobayashi 2002, unpublished data). The solid line is used in the model simulations.

lation, but PAI'_{min} is necessary to describe transpiration. Here, PAI'_{min} denotes effective plant area index excluding leaves (stem and branch area) because it is difficult to measure the value of PAI'_{min} on LP, assuming that $PAI'_{min} = 0.8$ as the same value on LL.

Moisture availability, β_{soil}, is obtained using Eq. (24) for forest sites because there is an evergreen *Vaccinium* sp. on the forest floors. Although resistance r_g should be determined after consideration of *Vaccinium* sp. physiology, r_g is treated as constant because of insufficient knowledge of its physiology. Parameters of water storage capacity, which are related to interception (see Yamazaki 2001), are assumed to be equal for all sites to those obtained in the LL site because Toba and Ohta (2002) suggested that storage capacity does not depend on tree species in eastern Siberia. Minimum snow albedo A_{min} (see Yamazaki 2001) is set to 0.55 in order that simulated snow disappearance and albedo correspond to observations.

Initial conditions of snow and soil are given at around 20 April for each site and year. Observed snow water equivalent and density are used; soil temperature is given as an interpolation of measurements. For soil water content, a constant value of 0.2 is assumed for all sites except the LP site. Because soil in the pine site is relatively sandy and dry compared with other sites, the initial water content is assumed to be 0.1 in LP.

b. Diurnal variations of fluxes

Figure 3 shows a comparison of observed and calculated diurnal variations of heat fluxes in RG and LP. Figure 3a indicates the result of mature stage in RG on 3 July 2000. Here, the observed sensible and latent heat fluxes were based on Bowen ratio method. On the other hand, Fig. 3b shows that of 5 June 2000 in LP. Here, sensible and latent heat fluxes were measured by the eddy covariance method. Our model is able to simulate the characteristics of the diurnal variation of the fluxes. However, the phase of *G* in RG is shifted; a possible reason is that *G* was measured at 5-cm depth, not at the surface with a heat plate. See Yamazaki (2001) for examples of comparison of diurnal variations in LL.

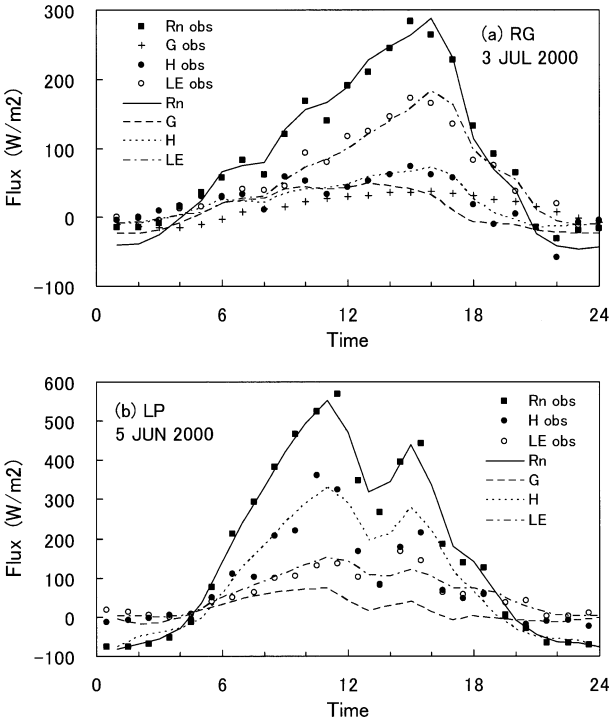

FIG. 3. Diurnal variation of energy fluxes: (a) RG on 3 Jul 2000 and (b) LP on 5 Jun 2000. Lines are simulation results; symbols are observations.

c. Seasonal variations of fluxes

Figure 4 shows simulated and observed Bowen ratio in RL, RG, and LP in 2000. Figure 5 shows simulated seasonal variations of (a) net radiation, (b) heat storage, (c) sensible heat, and (d) latent heat fluxes above the canopy in RL, RG, LL, and LP. In Fig. 5c, horizontal arrows denote the snow season (April) and leaf-out season (May–June); because pine is evergreen, no leaf-out season is given for LP. A no-grass-cutting simulation is also indicated by thin solid lines in Fig. 5 to examine the effect of grass cutting: all parameters, including PAI, are maintained after the cutting date (21 July, a vertical arrow in Fig. 5c). Figure 6 shows simulated seasonal variations of heat fluxes at the forest floor (in RL, LL, and LP) or on the soil surface (in RG). Characteristics of simulated fluxes at each site will be described hereafter.

The features of seasonal change at RL and LL are similar in 2000. During the snowmelt season, most incident energy is partitioned into sensible heat flux and heat flux into the ground, *G* (including energy to melt snow). This sensible heat flux from the forest is used to heat the atmosphere in the snowmelt season as pointed out by Yamazaki (1995). Sensible heat flux on the forest floor is downward in this season; thus it contributes to snowmelt. In the leaf-out season, latent heat flux increases rapidly and sensible heat flux decreases. After opening of leaves, sensible heat flux and latent heat flux

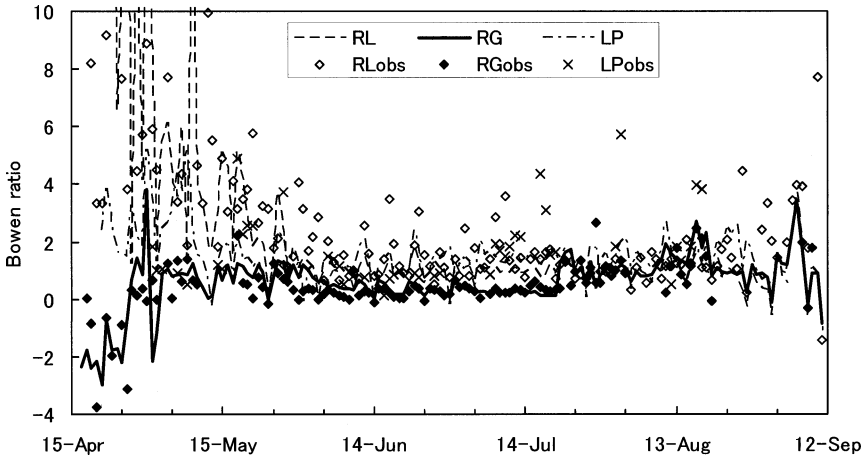

FIG. 4. Simulated and observed seasonal variation of Bowen ratio in RL, RG, and LP in 2000.

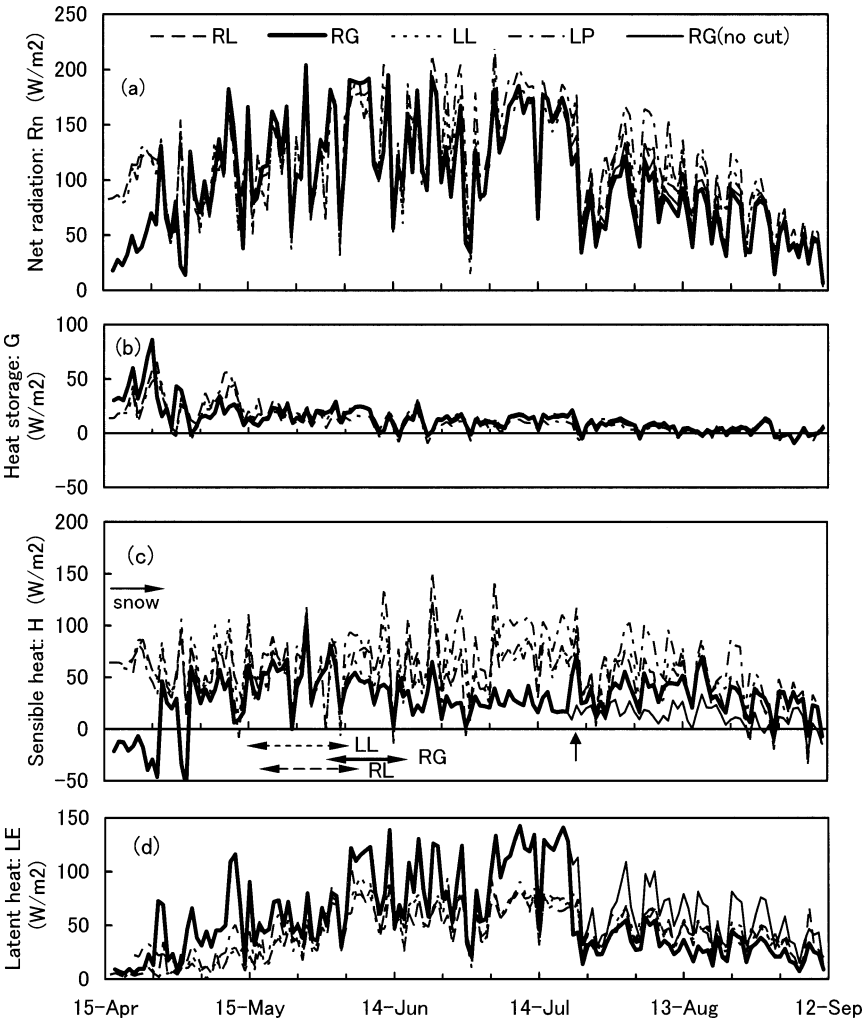

FIG. 5. Simulated seasonal variation of heat fluxes above the canopy in 2000: (a) net radiation, (b) heat storage, (c) sensible heat, and (d) latent heat flux. Also, the no-grass-cutting simulation is shown by the thin solid line. Horizontal arrows in (c) show the snow season (Apr) and leaf out (May–Jun). A vertical arrow in (c) is the date of grass cutting (21 Jul).

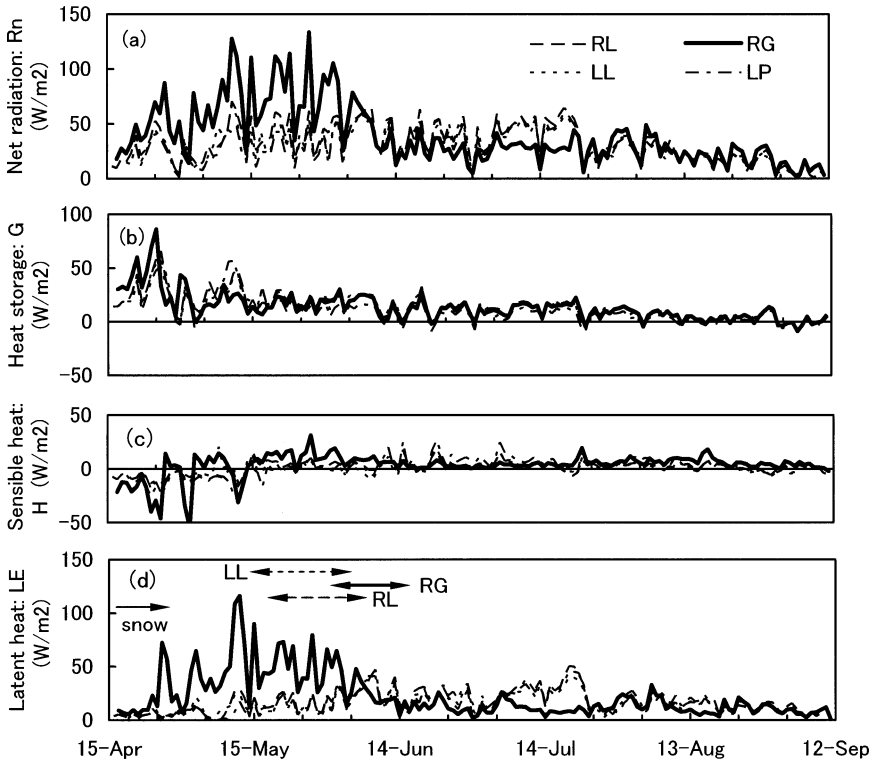

FIG. 6. Simulated seasonal variation of heat fluxes at forest floor (in RL, LL, and LP) or soil surface (in RG) in 2000.

have almost identical magnitude. These features of seasonal variation are found in simulations in LL1998 (Yamazaki 2001) and LL1999 (data not shown), and observation in LL1998 (Ohta et al. 2001).

At the grass site, RG, latent heat flux is dominant before grass cutting, with a Bowen ratio of 0.2 above the canopy. It should be noted that stomatal parameters are identical to those in forest sites, except for B (Table 2). Nevertheless, heat balances are markedly different between RG and the forest sites; this phenomenon will be discussed in the next section. The net radiation in the snow season is small compared with the forest sites because it is treated as a snow surface without canopy in this season. Sensible and latent heat fluxes are similar after grass cutting. The simulation that excludes grass cutting shows that the large latent heat flux persists after that date. In practice, actual latent heat flux seems to be smaller than the simulation because vegetation activity might decline in autumn. In any event, grass cutting's impact on the heat balance is clear. At the soil surface, net radiation and latent heat fluxes are large in the early season, but they decrease rapidly because transmitted radiation through the canopy decreases as grass grows and β_{soil} decreases as the soil becomes dry.

At the pine site, LP, seasonal change is similar to that at larch sites (LL and RL), However, net radiation is slightly larger than at other sites in July and August because of the low albedo. Moreover, latent heat flux increases just after snow disappearance because pine is an evergreen conifer. Corresponding to increasing latent heat flux, sensible heat flux in this season is small compared to larch sites. Sensible heat flux at the forest floor is nearly zero or negative (downward) after snowmelt season; it increases and changes to positive values in summer. In the period from 15 to 20 July, as the saturation deficit increases, latent heat flux decreases; this was also found in observations (Hamada et al. 2004). This behavior cannot be simulated if $B = 0.027$ (as with the larch). In August, sensible heat flux is larger than latent heat flux in this simulation; this also corresponds with observations. Observed maximum latent heat flux reaches 200 W m^{-2} in June, which is larger than the simulated value. One reason is that sometimes $H + LE > \text{Rn} - G$ for certain wind direction in this site (Hamada et al. 2004), but the simulation is balanced.

d. Water budget

Figure 7 shows the water budget from 21 April to 31 August in each site and year. Two bars are indicated for each site and year: the left one shows input containing precipitation in this period and snow at the beginning of the period. On the other hand, the right one shows evapotranspiration containing three components: interception, $E_{\text{intercept}}$; transpiration, E_{transpi}; and understory evapotranspiration, E_{under}.

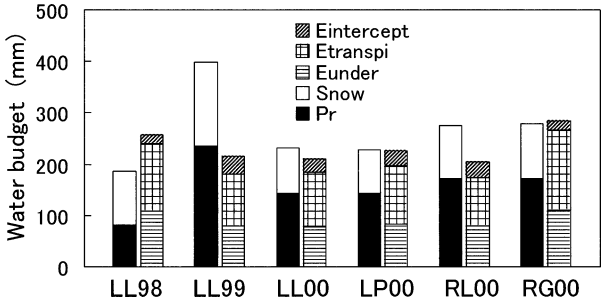

FIG. 7. Water budget from 21 Apr to 31 Aug for each site and year. The left bar in each site is input containing precipitation in this period and snow at 21 Apr. The right bar is evapotranspiration containing interception, transpiration, and understory evapotranspiration.

It was found that the input water varies greatly from year to year: less precipitation (82 mm) in 1998, more (236 mm) in 1999, and a normal amount (143 mm) in 2000 in LL (average precipitation from April to August is 139 mm in Yakutsk). However, total evapotranspiration varies in a small range of ~ 50 mm (maximum is 265 mm in 1988 and minimum is 211 mm in 2000) in LL. This is consistent with the suggestion that ice meltwater from deeper soil is transported upward and used for transpiration in dry summer according to stable isotopes analysis (Sugimoto et al. 2003).

The ratio of understory evapotranspiration to total evapotranspiration, $E_{\text{under}}/E_{\text{total}}$, distributes ranges between 0.37 (LL2000 and LP) and 0.44 (RG). The following ratios were reported in observation: 0.35 in the LL site in 1998 (Ohta et al. 2001) and 0.4 through 0.5 in the LP site (Hamada et al. 2004). Although $E_{\text{under}}/E_{\text{total}}$ is large in the pine forest according to observations, it is almost identical for each site and year in model calculations.

The ratio of interception to precipitation, $E_{\text{intercept}}$/Pr, is 0.15 through 0.21 in forest sites; the minimum is obtained in LL1999, and the maximum is in LL1998 and LP. In LL1999, the absolute value of $E_{\text{intercept}}$ is large (36 mm) but precipitation is larger; thus the ratio becomes small. According to observations, the ratio is 0.15 in LL1998 (Ohta et al. 2001) and approximately 0.3 in LP (Toba and Ohta 2002). On the other hand, the ratio is calculated as the small value of 0.11 in the RG site in this study. Parameters of water storage capacity were assumed to be the same for all sites. This is most likely not very realistic, and it will be necessary to investigate this further in future studies.

5. Discussion

a. Small Bowen ratio in RG

As shown in Fig. 4, the Bowen ratio (*H*/*LE*) in RG is markedly small compared to that in RL in midsummer. What explains this small Bowen ratio in RG? It is difficult to identify the reason from observations alone, but the model can be a powerful tool to investigate it. First, sensitivity of the heat balance on several parameters is investigated in RG to determine which parameter is dominant over heat balance. Next, the reason for the small Bowen ratio in RG is discussed according to the sensitivity test result.

The sensitivity test compares the average sensible and latent heat fluxes and Bowen ratio between 16 June (leaves grew) and 20 July (the day before grass cutting). Control run is defined as the run with standard parameters listed in Table 2. Heat balance responses are examined when one (or two) parameter(s) is (are) changed.

Sensitivity test results are shown in Table 3. Also, RL (control) is given for comparison. The difference of parameters between RG and RL is found in *h*, PAI_{max}, PAI_{min}, and *B*. Canopy height *h* is slightly uncertain in grassland; however, the dependence on *h* is small if PAI is conserved. Although the maximum plant area index, PAI_{max}, in RG is larger than in RL, if PAI_{max} is set equal to that of RL (1.1), the decrease of latent heat flux is limited. Furthermore, when PAI_{min} and PAI_{max} are set as in RL, the heat balance approximates that of RL. Parameter *B*, which is related to transpiration control with air dryness, is slightly smaller than that in forest sites. If *B* is set to 0.027 hPa^{-1}, the same as RL, evapotranspiration is too suppressed in the several days before grass cutting. It was hot and dry on those days, so transpiration seems to be slightly reduced in the observations. However, the seasonal change characteristics of the heat balance can be simulated even if a value of *B*

TABLE 3. Heat balance sensitivity to changes in parameters between 16 Jun and 20 Jul in RG; RL is given for comparison. Only the parameter listed in the ''changed parameter'' column is changed from the control (standard) run with parameters as in Table 2. Values in parentheses show the difference from the control run.

Changed parameter	*H* (W m^{-2})	*LE* (W m^{-2})	Bowen ratio
No change (control)	26	99	0.26
$h = 0.3$ m	27 (+1)	96 (−3)	0.28 (+0.02)
$\text{PAI}_{\text{max}} = 1.1$	38 (+12)	90 (−9)	0.42 (+0.16)
$\text{PAI}_{\text{max}} = 1.1$; $\text{PAI}_{\text{min}} = 0.75$	56 (+30)	70 (−29)	0.80 (+0.54)
$B = 0.027$	34 (+8)	89 (−9)	0.31 (+0.11)
$B = 0.014$	22 (−4)	103 (+5)	0.21 (−0.05)
$r_m = 100$ s m^{-1}	45 (+19)	77 (−22)	0.58 (+0.32)
RL (control)	61	61	1.00

TABLE 4. Potential evaporation (E_p and LE_p), modeled actual evaporation (LE), and measured precipitation (Pr) in the warm season. The normalized quantities (E/E_p and Pr/E_p) indicate the stength of biophysical control that each vegetation type exerts on the climate system. The data period is shown in Table 1.

Site year	Effective days	E_p (mm, mm day^{-1})	LE_p (W m^{-2})	LE (W m^{-2})	E/E_p	Pr (mm)	Pr/E_p
RL2000	149	572, 3.84	111.1	41.5	0.374	191	0.334
RG2000	148	539, 3.64	105.4	54.4	0.516	191	0.354
LL1998	148	729, 4.93	142.5	51.7	0.363	106	0.145
LL1999	145	602, 4.15	120.1	44.5	0.370	255	0.424
LL2000	139	572, 4.12	119.1	43.9	0.369	145	0.253
LP2000	126	549, 4.36	126.1	52.3	0.415	145	0.264

as for RL is used. Impact of r_m change is considerable; although we can obtain a similar Bowen ratio using $r_m = 100$ s m^{-1} with a small value of B (e.g., 0.014 hPa^{-1}), the shape of the seasonal changes becomes different.

As a result, the plant area index ($\mathrm{PAI_{min}}$ and $\mathrm{PAI_{max}}$) is very important to simulate a small Bowen ratio in the grassland site (RG). This indicates that contributory plant area to transpiration, or leaf area, $\mathrm{PAI_{max}} - \mathrm{PAI_{min}}$, is as significant as total plant area index. In other words, because leaf area, not including stem and branch areas, is small in Siberian forests (large $\mathrm{PAI_{min}}$), forest evapotranspiration is limited compared with grassland having a similar plant area index. It is not necessary that parameters related to stomatal resistance are changed between forest and grasslands to simulate the seasonal course of heat balance variation in our model, at least in this study region. Note that when using a model that does not distinguish leaf area from stem and branch area, such as the big leaf model, resistance or other parameters prescribing evapotranspiration might differ for forest and grasslands.

b. Potential evaporation

Potential evaporation is a useful index to discuss climatological condition of water and energy balances. For example, although latent heat flux increases and the Bowen ratio decreases in spring, it is difficult to judge whether the reason is only temperature dependency of the Bowen ratio or vegetation activity. If potential evaporation completely depends on only climate, evapotranspiration normalized by the potential evaporation depends on only surface (soil/vegetation) condition. However, most concepts of potential evaporation (e.g., Penman's formula) use net radiation, which depends on surface condition (e.g., albedo).

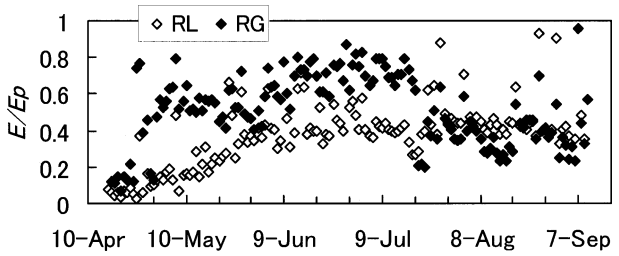

FIG. 8. Daily evapotranspiration normalized by potential evaporation in RL and RG in 2000.

In this study, the definition proposed by Kondo and Xu (1997) is introduced [English description is found in Xu and Haginoya (2001)]. According to Kondo and Xu (1997), potential evaporation is defined as evaporation from a virtual saturated surface with roughness of 0.005 m, albedo of 0.06, and emissivity of 0.98. This potential evaporation is easily calculated from incoming shortwave and longwave radiation, air temperature, humidity, and wind speed. Because surface condition is fixed and incoming radiation is input instead of net radiation, the new potential evaporation exactly reflects climate. For example, let us compare potential evaporations of Kondo and Xu (1997), E_{pK}, and Penman (1948), E_{pP}, for RL and RG sites. These two sites are very near, so the difference of meteorological condition is small. Thus potential evaporations as a climatic index should be close for both sites. Differences of E_{pK} between RL and RG is only 0.2 mm day^{-1} (will be presented in Table 4); however, E_{pP}, which is calculated with observed net radiation, induces difference of 0.6 mm day^{-1}. Coefficient of correlation between E_{pK} and E_{pP} on each site is higher than 0.95 on daily basis. Linear regression equations are $E_{pP} = 1.0484E_{pK} + 0.2212$ in RL and $E_{pP} = 0.973E_{pK} + 0.0748$ in RG, respectively, where the units of E_p are millimeters per day. The values of E_{pK} and E_{pP} are close to each other in RG, but E_{pP} is larger than E_{pK} by 10% in RL.

Figure 8 shows seasonal change of daily evapotranspiration normalized by potential evaporation, E/E_p in RL and RG. In the RL site, E/E_p is 0.1 in the leafless season; then it increases rapidly to 0.4 after leaf out. This behavior is common to both RL and LL (figure is omitted for LL). Sometimes E/E_p spikes irregularly above 0.6 because of rainfall. Conversely, in the LP site data (not shown), it is about 0.3 in spring; then it increases gradually to 0.4. In the RG site, the feature differs from forest sites: E/E_p reaches 0.7 before grass cutting and decreases around 0.4 after cutting. Because dependency of evaporation on meteorological conditions is removed by means of normalizing by E_p, the gap around 20 July is caused solely by grass cutting. The value of E/E_p is as high as 0.5 or 0.6 between the snow disappearance (26 April) and the grass growing in RG, and it is low around 0.1 until the snow disap-

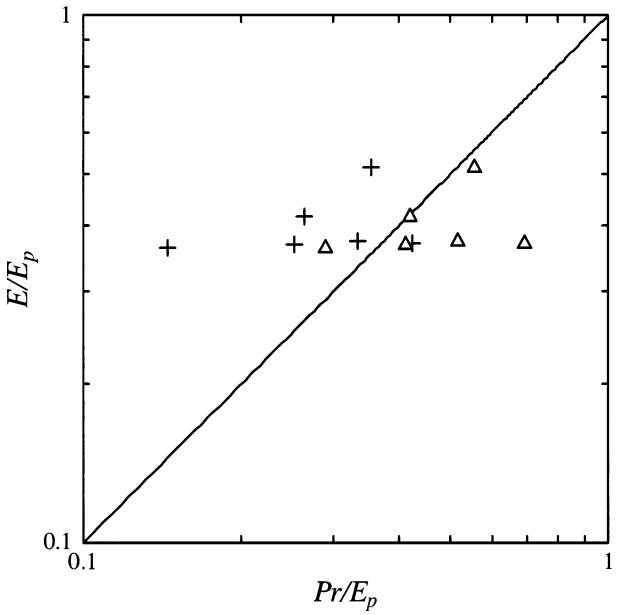

FIG. 9. The relationship between precipitation Pr and evapotranspiration E in warm season (shown in Table 4). Both Pr and E are normalized by potential evaporation. +: Pr is the only precipitation in the period; △: including snow at the end of Apr.

pearance. The reason is that the ground is treated as pure snow cover before the snow disappearance, and after that it is treated as a wet soil surface.

Table 4 summarizes seasonal totals and averages of potential evaporation and induced variables along with calculated evaporation by the model and measured precipitation in warm season. Figure 9 displays the relationship between Pr/E_p and E/E_p. The value of E/E_p in larch sites is almost constant at 0.37 independent of year, although precipitation varies widely from year to year. Thus it is confirmed that actual evapotranspiration can be estimated by calculating potential evaporation from meteorological data. In the pine forest (LP), E/E_p is 0.42; it is slightly larger than that in the larch sites. On the other hand, it is large, at 0.52, in the grassland (RG). The values of E/E_p in this study are small compared with those with typical temperate vegetation in the warm season, which are 0.7 or more (e.g., Kondo 1998). According to Fig. 9, plots distribute on the left of the one-to-one line (+). This means that the amount of evapotranspiration in the period is larger than the precipitation in the same period. One reason for this is that snowmelt water is used; however, if the amount of snow is added to the precipitation (△), some plots still locate on the left side of or near the one-to-one line. Because runoff is also present at least during the snowmelt season, the amount of water is insufficient in certain years. Melted water from the thawing of the soil or a horizontal transport of subsurface meltwater from neighboring areas satisfy the excess of evaporation, as implied by Fig. 7.

6. Conclusions

Water and energy exchanges were evaluated at ground surfaces covered by larch and pine forest, and grassland, in eastern Siberia using a one-dimensional land surface model. The main conclusions of this study are

1) Diurnal and seasonal variations of fluxes at all sites are reasonably simulated by using the same stomatal parameters except for the parameter for the influence of air dryness, B. Eventually the model, after having been tuned to the larch forest site, is able to predict time series of heat balance in other ecosystem sites in eastern Siberia. In the grassland site, the Bowen ratio of 0.2 is obtained in midsummer; it is smaller than that in forest sites (about 1). Sensitivity tests indicate that leaf area, which contributes to transpiration, should be given accurately along with the total plant area index including stem and branch area, which does not contribute to transpiration. If plant and leaf areas are given, the seasonal course of the heat balance can be simulated using the same stomatal parameters for forests and grassland sites with the model, at least in this study region.
2) Although precipitation input varies widely from 82 to 236 mm, calculated total evapotranspiration varies only with a range of 50 mm around 238 mm in the larch site. Understory evapotranspiration accounts for from 37% to 44% of total evapotranspiration; interception is 15% to 21% of precipitation.
3) Potential evaporation (Kondo and Xu 1997), which depends on only climatological condition, is introduced to clarify the influence of seasonal changes of vegetation status on water and energy exchange. This potential evaporation indicates similar values for the neighboring larch forest site and grassland site, while Penman's formula indicates larger value by 10% in the larch forest. Evapotranspiration normalized by the potential evaporation is 0.37 in larch sites almost independent of year, even though precipitation varies widely. On the other hand, normalized evapotranspiration is 0.52 in grasslands. In some sites, evapotranspiration exceeds precipitation even if snow is accounted for; it supports the conjecture that meltwater from the thawing of the soil satisfies the excess of evaporation.
4) It is not uncommon for grassland to be cut in this region in summer. The impact of this grass cutting on the surface heat budget is marked.

Finally, topics and issues that could be addressed in future studies were summarized. The soil submodel should be improved in some processes, for example, permeability to permafrost, root activity under low temperature, and representation of organic layer or moss layer. At the same time, the magnitude and time scales of spinup of land states (soil moisture) should be addressed. After these studies we plan to discuss soil moisture behavior with our model. In this study the same

parameters of water storage capacity are assumed to estimate interception at all sites. The impact of this assumption should be investigated. Spatial distribution of fluxes and/or effect of horizontal flow (advection) seem important because the test sites are located along the banks of a major river. Fortunately, some members related to GAME-Siberia are analyzing spatial distribution of fluxes with aircraft data. We think it is possible to discuss this problem in combination with these results. Aerodynamic conductance and canopy conductance are useful to compare evaporation rate with other studies. Relative magnitude and seasonal variation of these conductances should be evaluated.

Acknowledgments. We extend our appreciation to Prof. T. Yasunari of Nagoya University and Prof. B. Ivanov of the Institute for Biological Problems of Cryolithozone for allowing us the opportunity to investigate in Siberia. We also thank all members of the GAME-Siberia project, especially Hisanori Tanaka, for their suggestions and cooperation. Constructive and careful comments by Dr. K. E. Mitchell and three anonymous reviewers have been valuable for revising the manuscript.

REFERENCES

Baldocchi, D. D., F. M. Kelliher, T. A. Black, and P. Jarvis, 2000: Climate and vegetation controls on boreal zone energy exchange. *Global Change Biol.,* **6,** 69–83.

Clapp, R. B., and G. M. Hornberger, 1978: Empirical equations for some soil hydraulic properties. *Water Resour. Res.,* **14,** 601–604.

Eugster, W., and Coauthors, 2000: Land–atmosphere energy exchange in Arctic tundra and boreal forest: Available data and feedbacks to climate. *Global Change Biol.,* **6,** 84–115.

Fukuda, M., and T. Ishizaki, 1980: A simulation model for frost penetration beneath the ground on the basis of equilibrium surface temperatures (in Japanese with English summary). *Seppyo. J. Japan. Soc. Snow Ice,* **42,** 71–80.

Garratt, J. R., 1992: *The Atmospheric Boundary Layer*. Cambridge University Press, 316 pp.

Hamada, S., T. Ohta, T. Hiyama, T. Kuwada, A. Takahashi, and T. C. Maximov, 2004: Hydrometeorological behaviour of pine and larch forests in eastern Siberia. *Hydrol. Processes,* **18,** 23–39.

Ishii, Y., 2001: The outline of the field observation at the right bank of the Lena River. Activity Report of GAME-Siberia 2000, GAME Publication 26, 83–86.

Kelliher, F. M., R. Leuning, and E.-D. Schulze, 1993: Evaporation and canopy characteristics of coniferous forests and grasslands. *Oecologia,* **95,** 153–163.

——, and Coauthors, 1997: Evaporation from an eastern Siberian larch forest. *Agric. For. Meteor.,* **85,** 135–147.

Kondo, J., 1998: Dependence of evapotranspiration on the precipitation amount and leaf area index for various vegetated surfaces (in Japanese with English summary). *J. Japan Soc. Hydrol. Water Resour.,* **11,** 679–693.

——, and J. Xu, 1997: Potential evaporation and climatological wetness index (in Japanese). *Tenki,* **44,** 875–883.

——, N. Saigusa, and T. Sato, 1990: A parameterization of evaporation from bare soil surfaces. *J. Appl. Meteor.,* **29,** 385–389.

Ohta, T., T. Hiyama, H. Tanaka, T. Kuwada, T. Maximov, T. Ohata, and Y. Fukushima, 2001: Seasonal variation in the energy and water exchanges above and below a larch forest in eastern Siberia. *Hydrol. Processes,* **15,** 1459–1476.

Penman, H. L., 1948: Natural evaporation from open water, bare soil and grass. *Proc. Roy. Soc. London,* **A193,** 120–146.

Raupach, M. R., and A. S. Thom, 1981: Turbulence in and above plant canopies. *Annu. Rev. Fluid Mech.,* **13,** 97–129.

Sugimoto, A., N. Yanagisawa, D. Naito, N. Fujita, and T. C. Maximov, 2002: Importance of permafrost as a source of water for plants in east Siberian taiga. *Ecol. Res.,* **17,** 493–503.

——, and Coauthors, 2003: Characteristics of soil moisture in permafrost observed in east Siberian taiga with stable isotopes of water. *Hydrol. Processes,* **17,** 1073–1092.

Suzuki, R., T. Hiyama, J. Asanuma, and T. Ohata, 2004: Land surface identification near Yakutsk in eastern Siberia using video images taken from a hedgehopping aircraft. *Int. J. Remote Sens.,* in press.

Toba, T., and T. Ohta, 2002: Modeling the characteristics of interception loss in forests (in Japanese with English summary). *J. Japan. Soc. Hydrol. Water Resour.,* **15,** 345–362.

Turner, N. C., and J. E. Begg, 1973: Stomatal behavior and water status of maize, sorghum, and tobacco under field conditions. *Plant Physiol.,* **51,** 31–36.

Xu, J., and S. Haginoya, 2001: An estimation of heat and water balances in the Tibetan Plateau. *J. Meteor. Soc. Japan,* **79,** 485–504.

Yabuki, H., 2001a: Installation of automatic climate observation system to the young larch forest site at right bank of Lena River. Activity Report of GAME-Siberia 2000, GAME Publication 26, 87–88.

——, 2001b: Installation of automatic weather system to the alas site at right bank of Lena River. Activity Report of GAME-Siberia 2000, GAME Publication 26, 95–97.

Yamazaki, T., 1995: The influence of forests on atmospheric heating during the snowmelt season. *J. Appl. Meteor.,* **34,** 511–519.

——, 2001: A one-dimensional land surface model adaptable to intensely cold regions and its application in eastern Siberia. *J. Meteor. Soc. Japan,* **79,** 1107–1118.

——, J. Kondo, T. Watanabe, and T. Sato, 1992: A heat-balance model with a canopy of one or two layers and its application to field experiments. *J. Appl. Meteor.,* **31,** 86–103.